



Age and growth of *Astarte borealis* (Bivalvia) from the southwestern Baltic Sea using secondary ion mass spectrometry

David K. Moss¹ · Donna Surge² · Michael L. Zettler³ · Ian J. Orland^{4,5} · Alex Burnette² · Abby Fancher²

Received: 14 May 2021 / Accepted: 5 July 2021

© The Author(s), under exclusive licence to Springer-Verlag GmbH Germany, part of Springer Nature 2021

Abstract

Traditional isotope sclerochronology employing isotope ratio mass spectrometry has been used for decades to determine the periodicity of growth increment formation in marine organisms with accretionary growth. Despite its well-demonstrated capabilities, it is not without limitation. The most significant of these being the volume of carbonate powder required for analysis with conventional drill-sampling techniques, which limit sampling to early in ontogeny when growth is fast or to species that reach relatively large sizes. In species like *Astarte borealis* (Schumacher, 1817), a common component of Arctic boreal seas, traditional methods of increment analysis are difficult, because the species is typically long-lived, slow growing, and forms extremely narrowly spaced growth increments. Here, we use Secondary Ion Mass Spectrometry (SIMS) to analyze $\delta^{18}\text{O}$ in 10- μm -diameter spots and resolve the seasonal timing of growth increment formation in *Astarte borealis* in the southeastern Baltic Sea. In the individual sampled here, dark growth increments can form in either the fall, winter, or spring. Furthermore, growth increment data from two populations (RFP3S = 54.7967° N, 12.38787° E; WA = 54.86775° N, 14.09832° E) indicate that in the Baltic Sea, *A. borealis* is moderately long-lived (at least 43 years) and slow growing (von Bertalanffy k values 0.08 and 0.06). Our results demonstrate the potential of *A. borealis* to be a recorder of Baltic Sea seasonality over the past century using both live- and dead-collected shells, and also the ability of SIMS analysis to broaden the spectrum of bivalves used in sclerochronological work.

Introduction

Isotope sclerochronology can be useful in determining the lifespan and growth history of marine organisms with accretionary hard parts. Organisms like bivalves, corals, and fish record their age-at-size in the form of growth increments,

similar to the growth rings in trees. In bivalves, growth increments form in response to environmental and biological conditions and at several periodicities: daily, tidal, fortnightly, monthly, and annual (Barker 1964; Pannella and MacClintock 1968; Clark 1974; Pannella 1976; Jones et al. 1983; Goodwin et al. 2001). One method to determine the timing of these increments is to examine patterns in the variation of oxygen isotope ratios ($^{18}\text{O}/^{16}\text{O}$; reported here as $\delta^{18}\text{O}$ values) along the axis of maximum growth of the biogenic carbonate. Oxygen isotope ratios are, in part, a function of temperature and can show patterns reflecting seasonal variation, which can then be used to distinguish annual from non-annual growth increments (e.g., Jones and Quitmyer 1996; Schöne and Surge 2012). Identification of annual growth increments allows for an understanding of lifespan and growth rate.

Traditional methods of isotope sclerochronology employ a micromilling system fit with a silica carbide dental bit or tungsten carbide dental scriber point to extract carbonate powder for analysis via isotope ratio mass spectrometry (IRMS). Using a computerized system, the user is able to sample digitized paths of shell material perpendicular to

Responsible Editor: A. G. Checa.

Reviewers: undisclosed experts.

✉ David K. Moss
dxm112@shsu.edu

¹ Department of Environmental and Geosciences, Sam Houston State University, Huntsville, TX 77431, USA

² Department of Geological Sciences, University of North Carolina, Chapel Hill, NC 27599, USA

³ Leibniz-Institute for Baltic Sea Research, Rostock, Germany

⁴ WiscSIMS, Department of Geoscience, University of Wisconsin-Madison, Madison, WI, USA

⁵ Wisconsin Geological and Natural History Survey, University of Wisconsin-Madison, Madison, WI, USA

growth increments in cross-sections. Growth is fastest early in ontogeny, so sampling is typically focused on the youngest parts of shells to maximize the amount of carbonate powder drilled and to minimize time averaging. Except for techniques like incremental step drilling (e.g., Schöne et al. 2005a), where samples are only taken at the leading edge of the trench, it is often difficult to sample growth increments late in ontogeny as they are narrowly spaced and may exceed the width of the drill bit itself. In fast growing and/or large species, like *Mercenaria mercenaria* and *Arctica islandica*, this is typically not a problem (e.g., Weidman et al. 1994; Quitmyer et al. 1997; Surge and Walker 2006; Surge et al. 2007; Schöne 2013), but it can become an issue in small, slow growing, long-lived species, like those from the genus *Astarte*.

Our Previous work used the traditional micromilling techniques to identify annual growth increments in the shells of *Astarte borealis* (Schumacher 1817) from the White Sea, Russia, where individuals reach 35.5 mm in length (Moss et al. 2018). There, individuals grow relatively slowly, experience growth slow-downs in the summer months that result in annual increment formation, and can live for at least 48 years. Such impressive longevity is not unusual for a high-latitude species, as across the Bivalvia there is a tendency for lifespan to increase and growth rate to decrease with higher latitude (Moss et al. 2016), though the pattern is often complex (Reed et al. 2021). *Astarte borealis* is a common component of many Arctic and boreal seas, so understanding its life-history strategy across its distribution will provide further understanding of high-latitude ecosystems and perhaps identify areas where it can be used as a biomonitor (e.g., Boening 1999; Dunca et al. 2005; Gillikin et al. 2005; Black et al. 2017). Though *A. borealis* from the White Sea experiences summer growth slow downs, it is not uncommon in bivalves and some gastropods that the timing of annual increment formation varies with latitude within a species (e.g., Jones et al. 1989; Quitmyer et al. 1997; Elliott et al. 2003; Surge et al. 2013); this could also be confirmed in *A. borealis* by comparing oxygen isotope ratios in different populations. One impediment to this end is that the size of *A. borealis* varies throughout its distribution. For example, individuals from the White Sea (max 35.5 mm length; Moss et al. 2018) are typically bigger than those from the Baltic Sea (max 28.7 mm length; Zettler 2002). However, because Baltic Sea *A. borealis* are smaller than their northern counterparts, traditional micromilling techniques cannot be used to identify the seasonal timing of annual growth increments or evaluate whether the season of slowed growth is similar to *A. borealis* from the White Sea or more typical of other bivalve and limpet species inhabiting cold-temperate to boreal biogeographic zones. Here, we employ secondary ion mass spectrometry (SIMS) to overcome this issue. SIMS allows for a horizontal sampling resolution of 10 µm

with a sampled mass of approximately a nanogram, orders of magnitude smaller than traditional micromilling and IRMS methods. SIMS has been applied to modern marine bivalves (e.g., Dunca et al. 2009; Olson et al. 2012; Vihtakari et al. 2016), as well as to both modern and fossil marine organisms that accrete carbonate hard parts (e.g., Kozdon et al. 2009; Matta et al. 2013; Helser et al. 2018a, b; Linzmeier et al. 2018; Wycech et al. 2018). Using this technique, here, we find that annual growth slow downs, which result in the formation of dark growth increments as viewed in cross-section, can occur in fall, winter, or spring (like many other bivalves from cold-temperate to boreal habitats but unlike *A. borealis* from the White Sea) and that individuals from the Baltic Sea are quite long-lived (up to 43 years) and slow growing.

Ecology

The aragonite bivalve *A. borealis* has a circumpolar panarctic distribution. In the Atlantic Ocean it has been reported from Newfoundland to Massachusetts Bay and Greenland to Iceland. It is also found along the Pacific Coast of Alaska and British Columbia, as well as the Arctic Seas around Russia and in the Baltic Sea from Germany to Poland (Zettler 2001). *Astarte borealis* is an extremely shallow burrower and is an infaunal suspension feeder. It prefers substrates of muddy-sand containing gravel (Saleuddin 1965) and is typically found between 0 and 300 m water depth (Zettler 2002). Due to low salinities and brackish waters in some areas of the Baltic Sea (e.g., Bornholm Basin, eastern Gotland Basin), *A. borealis* lives in deeper regions with higher salinity. The optimal salinity range lies between 14 and 30 practical salinity units (psu) (Oertzen 1973). It can survive in salinities between 10 and 15 psu with its minimum tolerance at 6–8 psu. In the Baltic Sea, densities of up to 1000 individuals/m² and a wet weight up to 1.3 kg/m² (or 80 g/m² ash-free dry weight) were observed (unpublished data from the IOW Benthos Data Base, Leibniz Institute for Baltic Sea Research Warnemünde). Compared to other areas of origin, the spawning season of *A. borealis* in the Baltic Sea shows an extremely long period of mature eggs and sperm, with a maximum in winter and spring season (Oertzen 1972).

Materials and methods

Study area

Samples used in our analysis were collected alive by one of the authors from 2001 to 2003 for use in the previous studies to understand the benthic ecology and distribution of marine species in the Baltic Sea (Zettler 2002). We focused

our efforts on two closely spaced localities from different depths in the southwestern Baltic Sea (Fig. 1); RFP3S, depth = 20.9 m, salinity = 16.7 psu, WA, depth = 31.3 m, salinity = 8.3 psu. Samples were collected with a van Veen grab. Biological tissue was preserved in the samples, but was removed for sclerochronologic analyses. The samples were first fixed on board in formaldehyde (4%) and later stored in ethanol (70%). Shell height (anterior to posterior) measurements were made using a digital caliper (to one significant digit) to compare sizes of individuals between the two populations examined here and also other studied populations.

Shell preparation and oxygen isotope analysis

Aragonite shells were cut along the maximum axis of growth to reveal growth increments (Fig. 2). One specimen was selected from the RFP3S population for SIMS analysis (specimen number RFP3S-59) and cast in a 2.5 cm-diameter and 4 mm-thick round epoxy mount along with multiple grains of the calcite standard UWC-3 ($\delta^{18}\text{O} = 12.49\text{‰}$ Vienna Standard Mean Ocean Water, VSMOW; Kozdon et al. 2009). The mount was sent to Wagner Petrographic for polishing down to 0.05 μm grit using a diamond polishing compound after which it was sputter coated with gold ~ 60 nm thick prior to SIMS analysis.

SIMS analysis was completed at the University of Wisconsin-Madison WiscSIMS lab on a Cameca IMS 1280. Instrumental parameters followed Wycech et al. (2018). A 1.0 nA primary beam of $^{133}\text{Cs}^+$ sputtered analysis pits ~ 10 μm in diameter and ~ 1 μm deep. Sputtered

secondary ions of $^{16}\text{O}^-$, $^{18}\text{O}^-$, and $^{16}\text{OH}^-$ were detected simultaneously on three Faraday detectors, with secondary $^{16}\text{O}^-$ count rates of ~ 2.4 Gcps. Oxygen isotope ratios ($\delta^{18}\text{O}$) of the shell are reported in permil units (‰) relative to the VPDB (Vienna Pee Dee Belemnite) standard. Precision was calculated as the 2 s.d. of repeated groups of bracketing measurements on the calcite running standard UWC-3, which averaged $\pm 0.24\text{‰}$ (2 s.d.) across the analysis session. For each group of 10–15 aragonite sample analyses, measured (raw) values of $\delta^{18}\text{O}$ were corrected to the VPDB scale in three steps. First, the bracketing measurements of UWC-3 were used to calculate the instrumental bias of calcite on VSMOW scale. Then, an adjustment for the small difference in instrumental bias (0.88‰) between calcite and aragonite analysis was applied based on calibration analyses of aragonite standard UWArg-7 ($\delta^{18}\text{O} = 19.73\text{‰}$ VSMOW, Linzmeier et al. 2016) completed at the beginning of the analysis session. Finally, conversion from the VSMOW to the VPDB scale followed Coplen et al. (1993).

Sampling started within the middle microstructural layer ~ 8.5 mm from the umbo at approximately the 12th couplet of light and dark growth increments. The early portion of this shell was lost to taphonomic processes, which forced us to choose a location with more visible growth increments with adequate spacing. Sampling proceeded by manual site selection along growth direction. Adjustments in the location of sampling paths across growth increments were made to maintain perpendicular direction relative to growth lines (Fig. 3A). In addition, we analyzed a series of SIMS sample pits ($n = 8$) along a single growth line from the

Fig. 1 Location of the study sites in southwestern Baltic Sea region. RFP3S = 54.7967° N, 12.38787° E; WA = 54.86775° N, 14.09832° E. Shells were collected as part of a previous study (Zettler 2002)

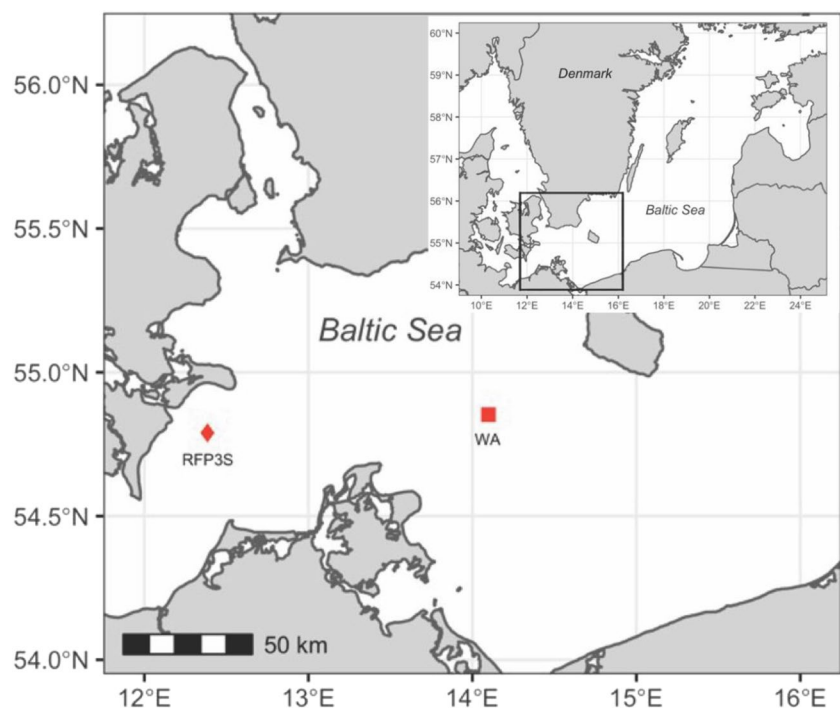


Fig. 2 Upper image shows axis of maximum growth in RFP3S-47. Lower image is polished cross-section stitched together using Olympus software. Direction of growth is from right to left in lower image. *OSL* outer shell layer, *MSL* middle shell layer, *ISL* inner shell layer

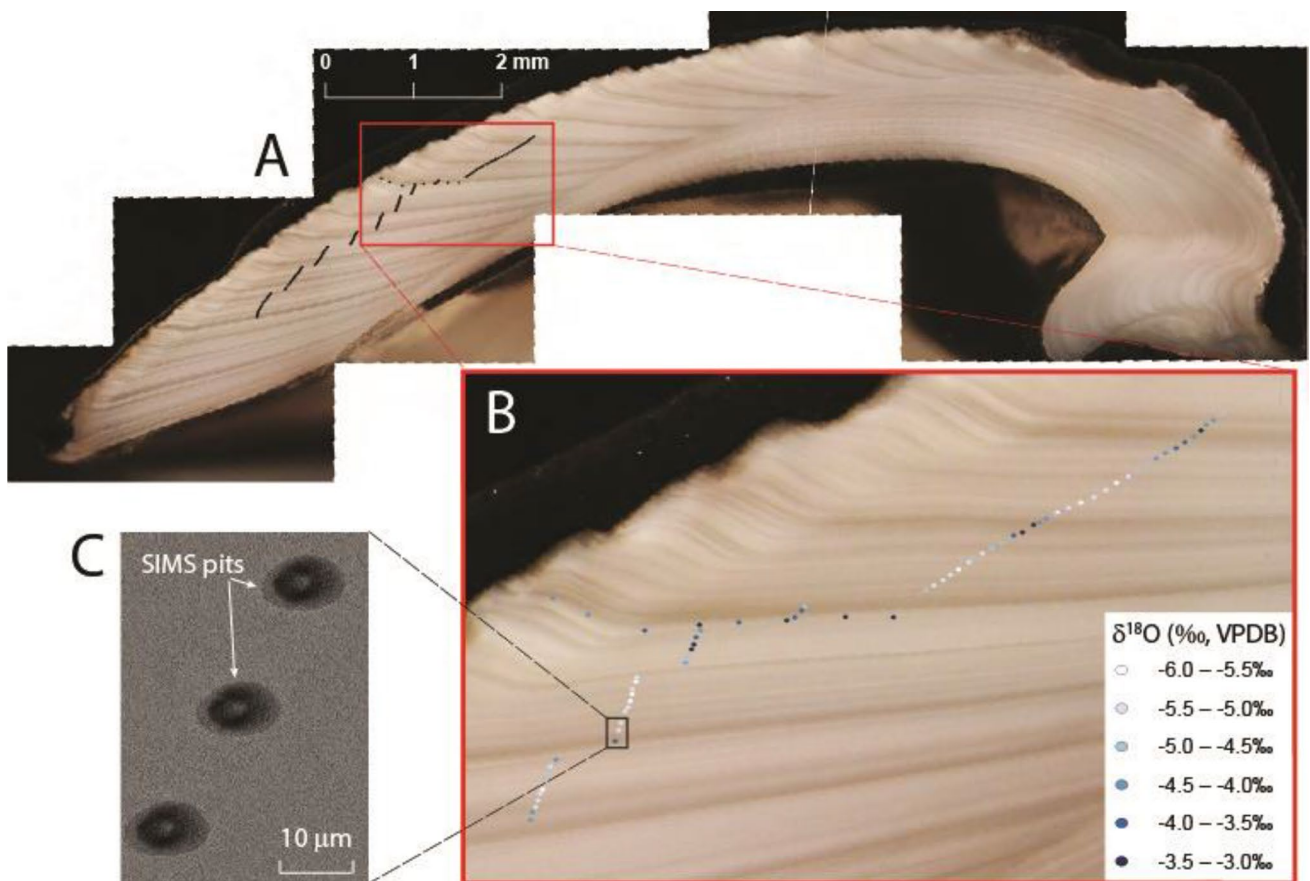
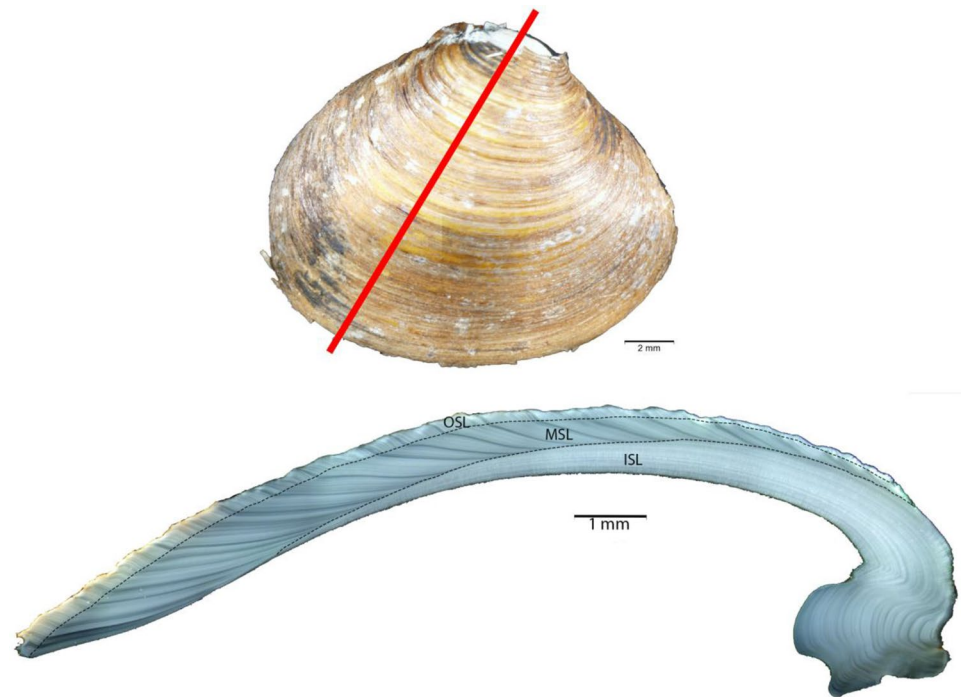


Fig. 3 Photomicrograph and SEM images showing SIMS pits along sampling paths and associated $\delta^{18}\text{O}$ values. **A** Cross-section shell image shows light and dark growth increments under reflected light. Black SIMS pits are enlarged from actual size to make them more visible. Growth direction is from right to left. Scale bar=2 mm. **B**

Enlarged image delineated by the red box on the shell cross-section showing color-coded ranges of SIMS $\delta^{18}\text{O}$ values in 0.5‰ intervals. The darker the blue, the higher the $\delta^{18}\text{O}$ values. **C** SEM images of SIMS sampling pits at high resolution (5.5 k magnification) showing examples with no irregularities. Scale bar=10 μ m

middle to outer microstructural layers representing coeval precipitation to evaluate lateral variability in oxygen isotope ratios (Fig. 3B). A total of 137 pits were generated representing ~4 mm of growth. See supplemental data archived in the Center for Open Source Science repository (<https://osf.io/>) for detailed reporting of all SIMS results.

After analysis, SIMS data were subjected to quality controls. First, analytical metrics of each sample measurement—including secondary ion yield, $^{16}\text{OH}^-/^{16}\text{O}^-$ ratio, and internal variability—were compared to the mean of the bracketing standards to confirm their quality. Scanning electron microscopy (SEM) of SIMS analysis pits were made to screen for irregular pit shapes that may bias the $\delta^{18}\text{O}$ data. The epoxy sample discs were mounted onto aluminum mounts with double-sided copper tape. Images were taken using a Zeiss Supra 25 FESEM operating at 5.5 kV, using the SE2 detector, 30 μm aperture, and working distances of 12–15 mm (Carl Zeiss Microscopy, LLC, Peabody, MA). SEM images of SIMS analysis pits revealed no irregularities of either pit morphology or aragonite substrate (Fig. 3C). In total, five SIMS spots were eliminated as outliers, and the remaining 132 are hereafter included in figures and discussion.

Next, we prepared the surface of specimen number RFP3S-59 for micromilling and traditional IRMS analysis as a coarse comparison to the ultra-high-resolution SIMS data. The specimen was repolished on a Buehler MetaServ 2000 variable speed grinder-polisher using diamond suspension solutions of 6 and 1 μm to remove the gold coating. Micromilling was performed on a Merchantek micromilling system fitted with a Brasseler tungsten carbide dental scriber point (part number H1621.11.008) and digitized paths followed 8 dark increments that overlapped the SIMS sampling path. Six of these samples yielded sufficient amounts of carbonate powder for analysis at the Environmental Isotope Laboratory, University of Arizona. Samples were reacted with dehydrated phosphoric acid under vacuum at 70 °C for 1 h and exolved CO_2 gas was analyzed with an auto carbonate reaction system (Kiel-III Devise) coupled to a Finnigan MAT 252 IRMS. Isotope ratios were calibrated based on repeated measurements of NBS-18 (National Bureau of Standards) and NBS-19, and no differential acid fractionation factor was applied to account for aragonite samples versus calcite standards. Precision is $\pm 0.1\text{‰}$ (1σ) for $\delta^{18}\text{O}$ values based on repeated measurement of internal carbonate standards. IRMS $\delta^{18}\text{O}$ values are also reported relative to the VPDB carbonate standard.

Visualization of growth increments

Thick sections of shells (approximately 1–2 cm) for all individuals from each population (RFP3S, $n = 67$; WA, $n = 40$) were made to visualize growth increments (Fig. 2).

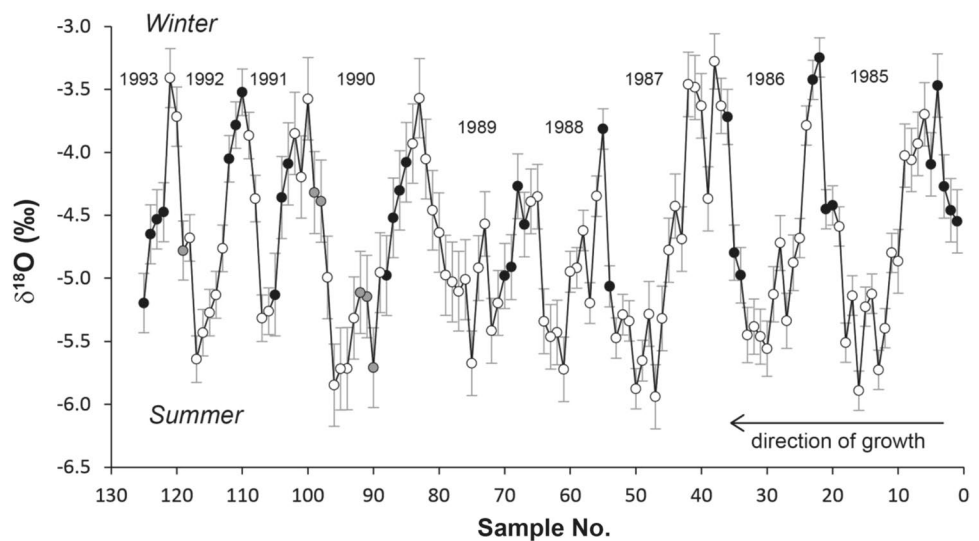
The shells of *A. borealis* are thin and delicate, so to prevent cracking during cutting, shells were first embedded with an epoxy. We experimented with two different epoxy materials. The first was Castolite AC from EagerPolymers (www.eagerpolymers.com). In this method, shells were placed in silicone muffin baking trays and covered in resin. The resin did not stick to the silicone surface, so embedded shells would come out easily. This approach proved successful in protecting the shells, but much resin was wasted as the muffin trays were larger than the shells themselves. To remedy this situation, we used a simple two-part syringe Gorilla Glue® clear epoxy and coated the shells in a single layer and then allowed them to cure on wax paper for twenty-four hours in a fume hood. After epoxy, shells were cut with Buehler Isomet low-speed saw along the axis of maximum growth to reveal internal increments. Thick sections of the shell were then glued onto a glass slide and polished on a Buehler MetaServ 2000 variable speed grinder-polisher by first using a 600 grit silicon carbide disc and finishing with diamond suspension solutions of 6 and 1 μm . Polished thick sections were imaged with an Olympus SZX7 stereomicroscope system coupled with an Olympus DP71 12.5 megapixel digital camera. A series of images were taken from umbo to commissure of each thick section and stitched together using Olympus Stream Essentials Software version 2.2. We then measured the cumulative widths of growth increments along the outer shell layer from umbo to commissure using Olympus Software. These widths were then transformed to a straight line distance by dividing each value by the total cumulative width and multiplying that by the overall shell height as measured using a digital caliper. This approach allows growth curves to be investigated in the context of shell heights measured for an entire population.

After all growth increments were measured for each population, we fit the von Bertalanffy growth equation (von Bertalanffy 1938, VBG) to the pooled size-at-age data using the non-linear least-squares (nls) procedure in the open source R language (cran.r-project.org). VBG describes the size of an individual at a given time (H_t)

$$H_t = H_\infty (1 - e^{-k(t-t_0)}),$$

where H_∞ = the asymptotic size, t_0 = the time at which $H_t = 0$, and k = the rate at which H_∞ is approached. The factor, k , is an important, but often misconstrued parameter of the VBG. In practice, a k value for any species of bivalve cannot be used to determine an exact amount of shell material accreted in a given year, because k is in units of year^{-1} . In addition, k is in part dependent on H_∞ so individuals with identical k values, but different H_∞ values would accrete different amounts of shell in a given year. Additionally, inverse plots of age versus cumulative size reveal that increments added throughout ontogeny decrease in their width at an

Fig. 4 SIMS $\delta^{18}\text{O}$ time-series in sample RFP3S-59 illustrating nine cycles labeled with years estimated from date of collection (± 2). Direction of growth is right to left on horizontal axis to match Fig. 3. Low $\delta^{18}\text{O}$ values correspond to warm temperature (summer), and higher values correspond to cooler temperature (winter). White circles are location of light increments. Black circles are location of dark growth increments. Gray circles in last four cycles on the left represent ambiguous increments. Error bars = 2σ



exponential rate. Thus, higher k values represent a faster approach to smaller growth increments.

Results

Oxygen isotope analyses

The SIMS $\delta^{18}\text{O}$ time-series of specimen RFP3S-59 exhibits a quasi-sinusoidal trend with relatively sharp peaks (high values) and valleys (low values) over nine clear cycles (Fig. 4). Values range from -5.9 to -3.3‰ and the average and 1 s.d. of the amplitude of the nine $\delta^{18}\text{O}$ cycles is $2.1 \pm 0.3\text{‰}$. The six IRMS $\delta^{18}\text{O}$ values that were sampled at a much coarser scale and centered on dark increments had notably higher $\delta^{18}\text{O}$ values ranging from -2.59 to -2.12‰ , with average and 1 s.d. of $-2.4 \pm 0.2\text{‰}$.

The lowest $\delta^{18}\text{O}$ values are consistently associated with light increments in the time-series measured by SIMS; however, the location of dark increments relative to the SIMS $\delta^{18}\text{O}$ time-series is more complicated (Figs. 3B, 4). Many of the dark increments coincide with higher $\delta^{18}\text{O}$ values, whereas some occur where values are increasing and others where values are decreasing. To test lateral variability, $\delta^{18}\text{O}$ values were measured in eight spots along a single growth increment from the middle to outer microstructural layer (Fig. 3B). Within the middle microstructural layer, $\delta^{18}\text{O}$ values ranged from -3.7 to -3.3‰ with an average of -3.4‰ ($n=6$) and spot-to-spot reproducibility ($\pm 0.3\text{‰}$ 2 s.d.) comparable to the running standard. The two $\delta^{18}\text{O}$ measurements in the outer microstructural layer were slightly more negative, each measuring -4.0‰ .

Size, lifespan, and growth

Measurements of shell height (Fig. 5A, B) showed no apparent differences in sizes between the RFP3S and WA populations. Our shell measurements compare well to those of previous studies in the Baltic Sea (Zettler 2002), though the smallest size fraction of our sample proved too difficult to work with for sclerochronologic studies, so they were not included.

Thin, dark, annual growth increments identified by their consistent occurrence at or near peak $\delta^{18}\text{O}$ values using SIMS allowed for the determination of lifespan and growth of each population. Because the two populations have similar size distributions, it was no surprise that their age distributions were similar, as well (Fig. 5C, D). In both populations, most individuals fall between 10 and 40 years in age at the time of collection, with peak abundances between 20 and 30 years. The maximum ages of each population are similar at 43 (RFP3S) and 41 (WA). In addition to similar age distributions, the VBG growth equations do not vary significantly either. Both populations have low k (0.08 RFP3S, and 0.06 WA) and H_∞ values (16.12 mm RFP3S, 19.81 mm WA) and thus exhibit relatively slow growth to a small size (Fig. 6).

Discussion

Annual growth checks

Isotope sclerochronology using IRMS analysis of $\delta^{18}\text{O}$ values has long been established as a reliable method for determining seasonal variation in growth rates of bivalve shells (e.g., Jones and Quitmyer 1996; references in Schöne and Surge, 2012). Our findings show that for bivalve shells that are small, slow growing, and long-lived and have extremely

Fig. 5 Histograms (counts) of shell heights and lifespans of individuals from RFP3S ($n=67$; **A, C**) and WA ($n=40$; **B, D**) populations

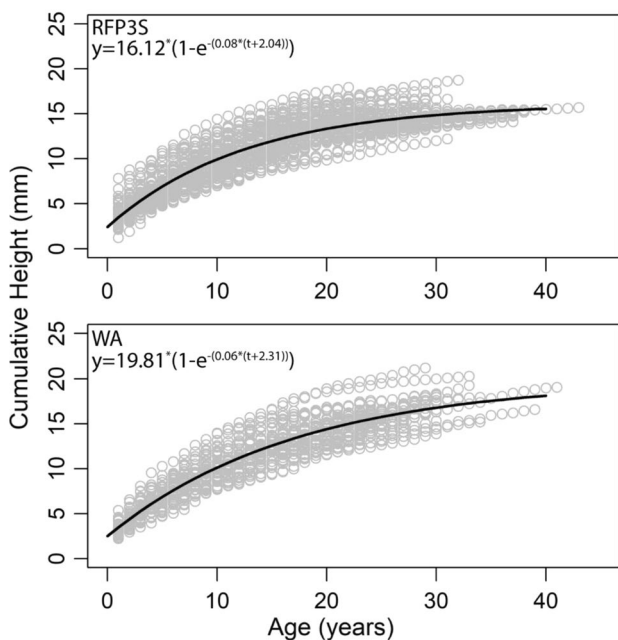
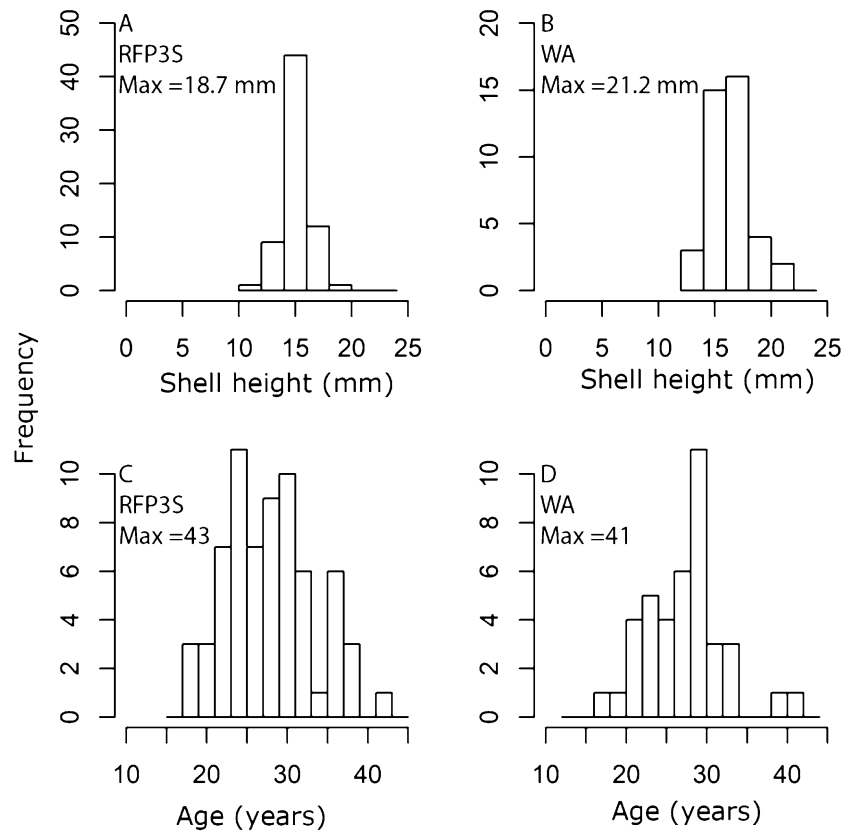


Fig. 6 von Bertalanffy growth equation fit to pooled age-at-size data for both populations investigated from the Baltic Sea. Black lines represent best fit VBG equations. Gray open circles represent cumulative size-at-age for each individual (RFP3S, $n=67$; WA, $n=40$) measured

narrowly spaced growth increments, that SIMS $\delta^{18}\text{O}$ analysis provides a reliable method for establishing seasonal growth checks and ontogenetic age that is otherwise unattainable. Oxygen isotope ratios sampled from the middle microstructural layer along a coeval growth line are statistically similar with a 2 s.d. comparable to the UWC-3 running standard. In comparison, the two samples taken from the outer microstructural layer were slightly more negative. Therefore, best SIMS practice is to test the variability along a coeval growth line, similar to a Hendy (1971) test in speleothems, and use that assessment to guide the time-series sampling in the direction of growth.

Our relatively small number of coarsely micromilled IRMS samples showed higher average $\delta^{18}\text{O}$ values compared to the SIMS $\delta^{18}\text{O}$ data. Although characterizing the cause of the offset between SIMS and IRMS $\delta^{18}\text{O}$ results is beyond the scope of this study, earlier studies have also documented offsets (also with SIMS $\delta^{18}\text{O}$ lower than IRMS $\delta^{18}\text{O}$) in low-temperature carbonates (Orland et al. 2015; Helsen et al. 2018b; Wycech et al. 2018). Helsen et al. (2018b) measured a $\sim 0.5\text{‰}$ offset in aragonitic fish otoliths, but found that SIMS more clearly captured seasonal $\delta^{18}\text{O}$ variation than micromilling/IRMS. Helsen et al. (2018b) also note a negative correlation of $^{16}\text{OH}^-/^{16}\text{O}^-$ and $\delta^{18}\text{O}$ values in SIMS measurements of their otolith and build on prior work (Orland et al. 2015; Wycech et al. 2018) in suggesting

that a possible cause of this correlation is the inclusion of water and/or organic matter in the sample; by this hypothesis, increased water and/or organic content would cause SIMS analyses to have lower $\delta^{18}\text{O}$ values. By nature of the analytical techniques, these components could be included in SIMS $\delta^{18}\text{O}$ measurements, but are excluded from IRMS. Interestingly, in this study, there is a weak positive correlation ($r^2=0.21$) of $^{16}\text{OH}^-/^{16}\text{O}^-$ and $\delta^{18}\text{O}$ values across all sample analyses. A notable exception to this trend is a strong negative correlation ($r^2=0.91$) of $^{16}\text{OH}^-/^{16}\text{O}^-$ and $\delta^{18}\text{O}$ values for the eight analyses along a single growth increment. No data exist, however, that quantitatively characterize the correlation of $\delta^{18}\text{O}$ and $^{16}\text{OH}^-/^{16}\text{O}^-$ or the $\delta^{18}\text{O}$ offset to water and/or organic inclusions, and establishing causation of these observations in SIMS analysis of biocarbonates is an ongoing challenge. Thus, the interpretations discussed below rely solely on the relative values and variability of SIMS $\delta^{18}\text{O}$ analyses and not the absolute $\delta^{18}\text{O}$ values. The quasi-sinusoidal trend in the SIMS $\delta^{18}\text{O}$ time-series likely reflects seasonal variation and demarcates annual changes in shell growth patterns representing 9 years of growth. Although difficult to quantify without detailed water temperature and $\delta^{18}\text{O}_{\text{water}}$ values during the growth period, we hypothesize that the seasonal signal likely reflects seasonal temperature change with lower $\delta^{18}\text{O}$ corresponding to summer growth. This will be the subject of a forthcoming paper. Several biological processes and environmental conditions have been reported to influence seasonal variation in shell growth, including reproduction/spawning, food supply, and minimum/maximum temperature thresholds lowering metabolic rates (e.g., Jones et al. 1983; Jones and Quitmyer 1996; Lutz and Rhoads 1980; Richardson 2001; Sato 1995; Schöne et al. 2005b). Shifts in the seasonal timing of slowed growth along a latitudinal gradient have been documented in many bivalve and limpet groups. Individuals collected along the eastern seaboard of the United States from Florida to New York (Jones et al. 1989; Quitmyer et al. 1997; Elliott et al. 2003) and along the eastern North Atlantic from northern Spain to Norway (Surge et al. 2013) form dark annual increments/growth checks during summer and those from mid to high latitudes form dark annual increments/growth checks during winter. The authors propose that temperature thresholds are the most likely explanation for the latitudinal shift in the timing of slowed growth. In a meta-analysis of bivalve growth seasonality, Killam and Clapham (2018) found that winter growth slow downs are common in polar bivalves, whereas summer slow downs are typical of mid-latitude species. This latitudinal pattern can be more complicated, however. Henry and Cerrato (2007) observed changes in the timing of dark increment formation in the northern hard clam, *Mercenaria mercenaria*, from Narragansett Bay, Rhode Island, USA, over a period of more than 2 decades. Earlier harvested individuals formed the expected dark increment

in winter, but the timing switched to a more complicated pattern with multiple dark increments in a single year. They hypothesized a human-induced change in environmental conditions within the watershed may be responsible for the more complicated growth pattern in *M. mercenaria* shells through time. The extremely long-lived ocean quahog, *Arctica islandica*, from the cold waters of the North Atlantic is known to form annual growth checks about 1 month after the maximum water temperature, but the time of formation depends on whether the individual lives above or below the thermocline (Schöne 2013). The timing of annual growth checks in this species can also be influenced by food availability, which becomes limited between fall and spring (Ballesta-Artero et al. 2017).

Moss et al. (2018) used isotope sclerochronology to decipher annual growth patterns in *A. borealis* from a population in the White Sea, Russia. There, clear couplets of light/dark increments were hypothesized to form annually and large enough to analyze using traditional micromilling/IRMS techniques. Despite the high-latitude, dark increments did not form in winter as expected and instead formed during summer. Using circumstantial evidence, Moss et al. (2018) reasoned that the most likely explanation for this unexpected pattern may correspond to the late summer spawning period in the White Sea. The specimen analyzed in our study from the Baltic Sea shows a more complicated pattern. Dark increments occur during cold or cool months (higher $\delta^{18}\text{O}$), and can begin formation during fall (years 1985–1988), winter (years 1989–1992), or spring (years 1990, 1991, and 1993) (Fig. 4). Summers (lower $\delta^{18}\text{O}$) are consistently associated with relatively wider, lighter colored growth increments that suggest faster growth, although light increments are also observed to commence in cooler months (cycles 1–4) and last into winter (cycles 5–9). Thus, temperature stress could explain the growth slow down in *A. borealis* from the Baltic Sea like it does in many bivalve species at high latitudes (Killam and Clapham 2018), but it likely is not the sole factor driving seasonal changes in growth rate. Spawning events can also result in annual increment formation, and *A. borealis* have been found with mature eggs and sperm in both winter and spring in the Baltic (Oertzen 1972), so that cannot be ruled out as a possibility. In addition, the individual sampled here appears to show a trend of seasonal slow downs shifting from fall to spring months later in ontogeny (Figs. 3, 4). Given the complicated timing of annual increments, we suggest that oxygen isotope data be collected from additional specimens to test these hypotheses.

Life history

Modern bivalves generally show an increase in lifespan and a decrease in von Bertalanffy k with latitude (Moss et al. 2016), a pattern that holds across Bivalvia and within

groups. Patterns within *A. borealis* appear to be more complex. Though this may be because methods for determining lifespans of *A. borealis* throughout its range are almost as varied as the reported lifespans themselves. At its northernmost limits, traditional isotope sclerochronology has shown *A. borealis* to be exceptionally long-lived, reaching 150 years in Greenland (Torres et al. 2011) and 48 years in the White Sea (Moss et al. 2018). Our measured ages of over 40 years in the Baltic Sea are not unexpected. To our knowledge, lifespans of *A. borealis* from the Baltic Sea have only been reported from Gusev and Rudinskaya (2014) at “greater than 10 years”. However, their study was not guided by isotope sclerochronology and their methods for determining annual growth increments are unclear. Elsewhere, several other studies have shown much shorter maximum lifespans (8–10 years) from the Sea of Okhotsk and the Eastern Siberian Sea (Gagayev 1989; Selin 2007, 2010). These studies though used ridges on the external shell surface instead of internal growth increments. External shell ridges are often problematic in determining lifespans of bivalves as they can be the result of disturbance events like storms, rather than from periodic events (Krantz et al. 1984).

Our results emphasize the need for using isotope sclerochronology to understand the true lifespan range of *A. borealis* throughout its distribution. While the traditional methods are often not possible on small, slow growing, and long-lived species, we demonstrate that SIMS provides a reliable method to determine the periodicity of growth increment formation. Furthermore, our data suggest that *A. borealis* could potentially act as not only a biomonitor, but also a climate recorder using both live- and dead-collected samples (Boening 1999; Szefer 2002) as the species has a long history in the Baltic Sea. The Baltic Sea has a long and complex anthropogenic pollution history and several short- and long-lived bivalves have contributed to understanding these patterns (Szefer and Szefer 1990; Rainbow et al. 2004; Liehr et al. 2005; Protasowicki et al. 2008; Hendozko et al. 2010; Schöne et al. 2021). Finally, while life-history information is available for a significant number of species, data currently appear to be skewed to larger, more commercially important groups. Oxygen isotope data determined using SIMS provide a mechanism to resolve this gap and to better understand benthic marine communities.

Acknowledgements We thank Garrett Braniecki for drafting the map figure. Comments from two anonymous reviewers improved the manuscript. Funding for this study was provided by the US National Science Foundation (NSF) to Surge (Grant #EAR-1656974). The WiscSIMS Laboratory is supported by the US NSF (Grant # EAR-1355590 and EAR-1658823).

Availability of data and materials The datasets generated during and/or analyzed during the current study will be made available in the Center for Open Science repository (<http://osf.io>).

Code availability. Not applicable.

Declarations

Conflict of interest The authors are not aware of any conflicts of interest which may arise as a result of this work.

References

- Ballesta-Artero I, Witbaard R, Carroll ML, van der Meer J (2017) Environmental factors regulating gaping activity of the bivalve *Arctica islandica* in Northern Norway. *Mar Bio* 164:116. <https://doi.org/10.1007/s00227-017-3144-7>
- Barker RM (1964) Microtextural variation in pelecypod shells. *Malacologia* 2:69–86
- Black HD, Andrus CFT, Lambert WJ, Rick TC, Gillikin DP (2017) $\delta^{15}\text{N}$ values in *Crassostrea virginica* shells provides early direct evidence for nitrogen loading to Chesapeake Bay. *Sci Rep* 7:3–10. <https://doi.org/10.1038/srep44241>
- Boening DW (1999) An evaluation of bivalves as biomonitors of heavy metals pollution in marine waters. *Environ Monit Assess* 55:459–470
- Clark GR (1974) Growth lines in invertebrate skeletons. *Annu Rev Earth Planet Sci* 2:77–99. <https://doi.org/10.1146/annurev.ea.02.050174.000453>
- Coplen TB, Kendall C, Hopple J (1983) Comparison of stable isotope reference samples. *Nature* 302:236–238
- Dunca E, Schöne BR, Mutvei H (2005) Freshwater bivalves tell of past climates: but how clearly do shells from polluted rivers speak? *Palaeogeogr Palaeoclimatol Palaeoecol* 228:43–57. <https://doi.org/10.1016/j.palaeo.2005.03.050>
- Dunca E, Mutvei H, Göransson P, Morth CM, Schöne BR, Whitehouse MJ, Elfman M, Baden SP (2009) Using ocean quahog (*Arctica islandica*) shells to reconstruct palaeoenvironment in Öresund, Kattegat and Skagerrak, Sweden. *Int J Earth Sci (geol Rundsch)* 98:3–17
- Elliot M, deMenocal PB, Linsley BK, Howe SS (2003) Environmental controls on the stable isotopic composition of *Mercenaria mercenaria*: potential application to paleoenvironmental studies. *Geochim Geophys* 4:1–16. <https://doi.org/10.1029/2002GC000425>
- Gagayev S (1989) Growth and production of mass species of bivalves in Chaun Bay (East Siberian Sea). *Oceanology* 29:504–507
- Gillikin DP, Dehairs F, Baeyens W, Navez J, Lorrain A, André L (2005) Inter- and intra-annual variations of Pb/Ca ratios in clam shells (*Mercenaria mercenaria*): a record of anthropogenic lead pollution? *Mar Pollut Bull* 50:1530–1540. <https://doi.org/10.1016/j.marpolbul.2005.06.020>
- Goodwin DH, Flessa KW, Schöne BR, Dettman DL, Schöne BR (2001) Cross-calibration of daily growth increments, stable isotope variation, and temperature in the Gulf of California bivalve mollusk *Chione cortezi*: implications for paleoenvironmental analysis. *Palaios* 16:387–398. [https://doi.org/10.1669/0883-1351\(2001\)016](https://doi.org/10.1669/0883-1351(2001)016)
- Gusev AA, Rudinskaya LV (2014) Shell form, growth, and production of *Astarte borealis* (Schumacher, 1817) (Astartidae, Bivalvia) in the southeastern Baltic Sea. *Oceanology* 54:458–464. <https://doi.org/10.1134/S0001437014040043>
- Helser T, Kastle C, Crowell A, Ushikubo T, Orland IJ, Kozdon R, Valley JW (2018a) A 200-year archaeozoological record of Pacific cod (*Gadus macrocephalus*) life history as revealed through ion microprobe oxygen isotope ratios in otoliths. *J Archaeol Sci Rep* 21:1236–1246. <https://doi.org/10.1016/j.jasrep.2017.06.037>

- Helser TE, Kastle CR, McKay JL, Orland IJ, Kozdon R, Valley JW (2018b) Evaluation of micromilling/conventional isotope ratio mass spectrometry and secondary ion mass spectrometry of $\delta^{18}\text{O}$ values in fish otoliths for sclerochronology. *Rapid Commun Mass Spectrom* 32:1781–1790. <https://doi.org/10.1002/rcm.8231>
- Hendozko E, Szefer P, Warzocha J (2010) Ecotoxicology and environmental safety heavy metals in *Macoma balthica* and extractable metals in sediments from the southern Baltic Sea. *Ecotoxicol Environ Saf* 73:152–163. <https://doi.org/10.1016/j.ecoenv.2009.09.006>
- Hendy CH (1971) The isotopic geochemistry of speleothems—I. The calculation of the effects of different modes of formation on the isotopic composition of speleothems and their applicability as paleoclimate indicators. *Geochim Cosmochim Acta* 35:801–824
- Henry KM, Cerrato RM (2007) The annual macroscopic growth pattern of the northern quahog [=hard clam, *Mercenaria mercenaria* (L.)], in Narragansett Bay, Rhode Island. *J Shellfish Res* 26:985–993. [https://doi.org/10.2983/0730-8000\(2007\)26\[985:tamgpo\]2.0.co;2](https://doi.org/10.2983/0730-8000(2007)26[985:tamgpo]2.0.co;2)
- Jones DS, Quitmyer IR (1996) Marking time with bivalve shells: oxygen isotopes and season of annual increment formation. *Palaios* 11:340. <https://doi.org/10.2307/3515244>
- Jones DS, Williams DF, Arthur MA (1983) Growth history and ecology of the Atlantic Surf Clam, *Spisula solidissima* (Dillwyn), as revealed by stable isotopes and annual shell increments. *J Exp Mar Biol Ecol* 73:225–242. [https://doi.org/10.1016/0022-0981\(83\)90049-7](https://doi.org/10.1016/0022-0981(83)90049-7)
- Jones DS, Arthur MA, Allard DJ (1989) Sclerochronological records of temperature and growth from shells of *Mercenaria mercenaria* from Narragansett Bay, Rhode Island. *Mar Biol* 102:225–234. <https://doi.org/10.1007/BF00428284>
- Killam DE, Clapham ME (2018) Identifying the ticks of bivalve shell clocks: seasonal growth in relation to temperature and food supply. *Palaios* 33:228–236. <https://doi.org/10.2110/palo.2017.072>
- Kozdon R, Ushikubo T, Kita NT, Spicuzza MJ, Valley JW (2009) Intratest oxygen isotope variability in the planktonic foraminifer *N. pachyderma*: real vs. apparent vital effects by ion microprobe. *Chem Geol* 258(34):327–337
- Krantz DE, Jones DS, Williams DF (1984) Growth rates of the sea scallop, *Placopecten magellanicus*, determined from the $^{18}\text{O}/^{16}\text{O}$ record in shell calcite. *Biol Bull* 167:186–199
- Liehr G, Zettler ML, Leipe T, Witt G (2005) The ocean quahog *Arctica islandica* L.—a bioindicator for contaminated sediments. *Mar Biol* 147:671–679
- Linzmeier BJ, Kozdon R, Peters SE, Valley JW (2016) Oxygen isotope variability within *Nautilus* shell growth bands. *PLoS ONE* 11(4):e0153890. <https://doi.org/10.1371/journal.pone.0153890>
- Linzmeier ABJ, Landman NH, Peters SE, Kozdon R, Kitajima K (2018) Ion microprobe—measured stable isotope evidence for ammonite habitat and life mode during early ontogeny. *Paleobiology* 44:684–708. <https://doi.org/10.1017/pab.2018.21>
- Lutz RA, Rhoads DC (1980) Growth patterns within the molluscan shell. In: Rhoads DC, Lutz RA (eds) *Skeletal growth of aquatic organisms*. Plenum Press, New York, pp 203–254
- Matta ME, Orland IJ, Ushikubo T, Helser TE, Black BA, Valley JW (2013) Otolith oxygen isotopes measured by high-precision secondary ion mass spectrometry reflect life history of a yellow fin sole (*Limanda aspera*). *Rapid Commun Mass Spectrom* 27:691–699. <https://doi.org/10.1002/rcm.6502>
- Moss DK, Ivany LC, Judd EJ, Cummings PW, Bearden CE, Kim WJ, Artruc EG, Driscoll JR (2016) Lifespan, growth rate, and body size across latitude in marine Bivalvia, with implications for Phanerozoic evolution. *Proc R Soc B Biol Sci* 283:20161364. <https://doi.org/10.1098/rspb.2016.1364>
- Moss DK, Surge D, Khaitov V (2018) Lifespan and growth of *Astarte borealis* (Bivalvia) from Kandalaksha Gulf, White Sea, Russia. *Polar Biol* 41:1359–1369. <https://doi.org/10.1007/s00300-018-2290-9>
- Olson IC, Kozdon R, Valley JW, Gilbert PUPA (2012) Mollusk shell nacre ultrastructure correlates with environmental temperature and pressure. *J Am Chem Soc* 134:7351–7358
- Orland IJ, Kozdon R, Linzmeier B, Wycech J, Sliwinski M, Kitajima K, Kita N, Valley JW (2015) Enhancing the accuracy of carbonate $\delta^{18}\text{O}$ and $\delta^{13}\text{C}$ measurements by SIMS. American Geophysical Union, Fall Meeting, December 18, 2015. Presentation PP52B-03. <https://agu.confex.com/agu/fm15/meetingapp.cgi/Paper/67486>. Accessed 12 Apr 2021
- Pannella G (1976) Tidal growth patterns in recent and fossil mollusk bivalve shells. *Sci Nat Heidelberg* 63:539–543
- Pannella G, MacClintock C (1968) Biological and environmental rhythms reflected in molluscan shell growth. *Paleontol Soc Mem* 2:64–80
- Protasowicki M, Dural M, Jaremek J (2008) Trace metals in the shells of blue mussels (*Mytilus edulis*) from the Poland coast of Baltic sea. *Environ Monit Assess* 141:329–337. <https://doi.org/10.1007/s10661-007-9899-4>
- Quitmyer IR, Jones DS, Arnold WS (1997) The sclerochronology of hard clams, *Mercenaria* spp., from the South-Eastern USA: a method of elucidating the zooarchaeological records of seasonal resource procurement and seasonality in prehistoric shell middens. *J Archaeol Sci* 24:825–840. <https://doi.org/10.1006/jasc.1996.0163>
- Rainbow PS, Fialkowski W, Sokolowski A, Smith BD, Wolowicz M (2004) Geographical and seasonal variation of trace metal bioavailabilities in the Gulf of Gdansk, Baltic Sea using mussels (*Mytilus trossulus*) and barnacles (*Balanus improvisus*) as biomonitors. *Mar Biol* 144:271–286. <https://doi.org/10.1007/s00227-003-1197-2>
- Reed AJ, Godbold JA, Grange LJ, Solan M (2021) Growth of marine ectotherms is regionally constrained and asymmetric with latitude. *Global Ecol Biogeogr*. <https://doi.org/10.1111/geb.13245>
- Richardson CA (2001) Molluscs as archives of environmental change. *Oceanogr Mar Biol* 39:103–164
- Saleuddin ASM (1965) The mode of life and functional anatomy of *Astarte* spp. (Eulamellibranchia). *J Molluscan Stud* 36:229–257. <https://doi.org/10.1093/oxfordjournals.mollus.a064952>
- Sato S (1995) Spawning periodicity and shell microgrowth patterns of the venerid bivalve *Phacosoma japonicum* (Reeve, 1850). *Veliger* 38:61–72
- Schöne BR (2013) *Arctica islandica* (Bivalvia): A unique paleoenvironmental archive of the northern North Atlantic Ocean. *Glob Planet Chang* 111:199–225. <https://doi.org/10.1016/j.gloplacha.2013.09.013>
- Schöne BR, Surge D (2012) Bivalve sclerochronology and geochemistry. In: Seldon P, Hardesty J, Carter JG, coordinator (eds) Part N, Bivalvia, Revised, Volume 1 Treatise Online 46:14, 1–24. University of Kansas, Paleontological Institute, Lawrence, Kansas
- Schöne BR, Fiebig J, Pfeiffer M, Gleß R, Hickson J, Johnson ALA, Dreyer W, Oschmann W (2005a) Climate records from a bivalved Methuselah (*Arctica islandica*, Mollusca; Iceland). *Palaeogeogr Palaeoclimatol Palaeoecol* 228:130–148. <https://doi.org/10.1016/j.palaeo.2005.03.049>
- Schöne BR, Houk SD, Freyre Castro AD, Fiebig J, Oschmann W, Kröncke I, Dreyer W, Gosselck F (2005b) Daily growth rates in shells of *Arctica islandica*: assessing sub-seasonal environmental controls on a long-lived bivalve mollusk. *Palaios* 20:78–92
- Schöne BR, Huang X, Zettler ML, Zhao L, Mertz R, Jochum KP, Walliser EO (2021) Mn/Ca in shells of *Arctica islandica* (Baltic Sea)—a potential proxy for ocean hypoxia? *Est Coast Shelf Sci* 251:107257

- Schumacher CF (1817) Essai d'un nouveau système des habitations des vers testacés. Schultz, Copenhagen
- Selin NI (2007) Shell form, growth and life span of *Astarte arctica* and *A. borealis* (Mollusca: Bivalvia) from the subtidal zone of northeastern Sakhalin. *Russ J Mar Biol* 33:232–237. <https://doi.org/10.1134/S1063074007040050>
- Selin NI (2010) The growth and life span of bivalve mollusks at the northeastern coast of Sakhalin Island. *Russ J Mar Biol* 36:258–269. <https://doi.org/10.1134/S1063074010040048>
- Surge D, Walker KJ (2006) Geochemical variation in microstructural shell layers of the southern quahog (*Mercenaria campechiensis*): implications for reconstructing seasonality. *Palaeogeogr Palaeoclimatol Palaeoecol* 237:182–190. <https://doi.org/10.1016/j.palaeo.2005.11.016>
- Surge D, Kelly G, Arnold WS, Geiger SP, Gowert AE (2007) Isotope sclerochronology of *Mercenaria mercenaria*, *M. campechiensis*, and their natural hybrid form: Does genotype matter? *Palaios* 23:559–565. <https://doi.org/10.2110/palo.2007.p07-056r>
- Surge D, Wang T, Gutiérrez-Zugasti I, Kelley PH (2013) Isotope sclerochronology and season of annual growth line formation in limpet shells (*Patella vulgata*) from warm- and cold-temperate zones in the eastern North Atlantic. *Palaios* 28:386–393. <https://doi.org/10.2110/palo.2012.p12-038r>
- Szefer P (2002) Metal pollutants and radionuclides in the Baltic Sea—an overview. *Oceanologia* 44:129–178
- Szefer P, Szefer K (1990) Metals in molluscs and associated bottom sediments of the southern Baltic. *Helgol Meeresunters* 44:411–424
- Torres ME, Zima D, Falkner KK, Macdonald RW, O'Brien M, Schöne BR, Siferd T (2011) Hydrographic changes in Nares Strait (Canadian Arctic Archipelago) in recent decades based on $\delta^{18}\text{O}$ profiles of bivalve shells. *Arctic* 64:45–58. <https://doi.org/10.1016/j.jmb.2005.01.031>
- Vihtakari M, Renaud PE, Clarke LJ, Whitehouse MJ, Hop H, Carroll ML, Ambrose WG Jr (2016) Decoding the oxygen isotope signal for seasonal growth patterns in Arctic bivalves. *Palaeogeogr Palaeoclimatol Palaeoecol* 446:263–283
- von Bertalanffy L (1938) A quantitative theory of organic growth (Inquires on growth laws. II). *Hum Biol* 10:181–213
- von Oertzen J-A (1972) Cycles and rates of reproduction of six Baltic Sea bivalves of different zoogeographical origin. *Mar Biol* 14:143–149
- von Oertzen J-A (1973) Abiotic potency and physiological resistance of shallow and deep water bivalves. *Oikos Suppl* 15:261–266
- Weidman CR, Jones GA, Kyger (1994) The long-lived mollusc *Arctica islandica*: a new paleoceanographic tool for the reconstruction of bottom temperatures for the continental shelves of the northern North Atlantic Ocean. *J Geophys Res* 99:18305. <https://doi.org/10.1029/94JC01882>
- Wycech JB, Kelly DC, Kozdon R, Orland IJ, Spero HJ, Valley JW (2018) Comparison of $\delta^{18}\text{O}$ analyses on individual planktic foraminifer (*Orbulina universa*) shells by SIMS and gas-source mass spectrometry. *Chem Geol* 483:119–130. <https://doi.org/10.1016/j.chemgeo.2018.02.028>
- Zettler M (2001) Recent geographical distribution of the *Astarte borealis* species complex, its nomenclature and bibliography (Bivalvia: Astartidae). *Schr Malakozool* 18:1–14
- Zettler ML (2002) Ecological and morphological features of the bivalve *Astarte borealis* (Schumacher, 1817) in the Baltic Sea near its geographical range. *J Shellfish Res* 21:33–40

Publisher's Note Springer Nature remains neutral with regard to jurisdictional claims in published maps and institutional affiliations.